Environmental Pollution 256 (2020) 113419

Contents lists available at ScienceDirect

Environmental Pollution

journal homepage: www.elsevier.com/locate/envpol

Spatio-temporal evolution of ozone pollution and its influencing factors in the Beijing-Tianjin-Hebei Urban Agglomeration☆

Zhen-bo Wang [a, *], Jia-xin Li [a, b], Long-wu Liang [a, b]

[a] Institute of Geographic Sciences and Natural Resources Research, Chinese Academy of Sciences, 11A Datun Road, Chaoyang District, Beijing 100101, China
[b] College of Resources and Environment, University of Chinese Academy of Sciences, Beijing 100049, China

ARTICLE INFO

Article history:
Received 8 November 2018
Received in revised form
18 September 2019
Accepted 14 October 2019
Available online 23 October 2019

Keywords:
Beijing-Tianjin-Hebei urban agglomeration
Ozone pollution
Spatio-temporal changes
Influencing factors

ABSTRACT

Ozone has become a major atmospheric pollutant in China as the pattern of urban energy usage has changed and the number of motor vehicles has grown rapidly. The Beijing-Tianjin-Hebei Urban Agglomeration, also known as the Jing-Jin-Ji Urban Agglomeration (hereafter, JJJUA), with a precarious balance between protecting the ecological environment and sustaining economic development, is challenged by high levels of ozone pollution. Based on ozone observation data from 13 cities in the JJJUA from 2014 to 2017, the spatio-temporal trends in the evolution of ozone pollution and its associated influencing factors were analyzed using Moran's I Index, hot-spot analysis, and Geodetector using ArcGIS and SPSS software. Five key results were obtained. 1) There was an increase in the annual average ozone concentration, for the period 2014–2017. Comparing the 13 prefecture-level cities, ozone pollution in Chengde and Hengshui decreased, while it worsened in the remaining 11 cities. 2) Ozone pollution was worse in spring and summer than in autumn and winter; the peak ozone pollution season was from May to September; the average ozone concentration on workdays was higher than that on non-workdays, showing a counter-weekend effect. 3) Annual average concentrations were high in the central and southern parts of the study region but low in the north. 4) Prominent positive spatial correlations were observed in ozone concentration, with the best correlations shown in summer and autumn; concentrations were high in Baoding and Xingtai but low in Beijing and Chengde. 5) Concentrations of PM_{10}, NO_2, CO, SO_2, and $PM_{2.5}$, as well as average wind speed, sunshine duration, evaporation, precipitation, and temperature, all had significant effects on ozone pollution, and interactions between these influencing factors increased it.

1. Introduction

Ozone, as a greenhouse gas, plays a critical role in climate warming and is also a significant indicator of photochemical pollution (Wang et al., 2017). Due to its strong oxidizing properties, high ozone concentrations near the ground are hazardous to the human respiratory system, immune system, tissues, and organs such as the skin, which threatens health and even human life (Adams, 1987; Huan et al., 2018; Lefohn et al., 2016). In addition, ozone has adverse effects on social production and life. For instance, it affects the healthy growth of plants, resulting in reduced crop yields (Chameides et al., 1994; Feng et al., 2015; Tai et al., 2014), and it corrodes many metallic as well as non-metallic materials. In the 1940s and 1950s, serious photochemical smog in Los Angeles, USA led to an economic loss of USD 1.5 billion. More than 400 people aged over 65 died as a result of respiratory failure (Friend of Nature, 2001). Since then, photochemical smog incidents have occurred in major urban areas and industrial regions throughout the world (Cooper et al., 2014; Wang et al., 2017). The repeated and complicated characteristics of photochemical smog have made it difficult to control and, as a result, have attracted the attention of researchers (Yang et al., 2018); many countries and institutions collect monitoring data and conduct research regarding to ozone at ground level.

Ozone formation was initially characterized based on research into the occurrence of photochemical smog in Los Angeles. It is formed by the decomposition of nitrogen dioxide, aided by rapid conversion of nitric oxide to nitrogen dioxide in the presence of

☆ This paper has been recommended for acceptance by Charles Wong.

* Corresponding author.
E-mail addresses: wangzb@igsnrr.ac.cn (Z.-b. Wang), lijiaxin181@mails.ucas.ac.cn (J.-x. Li), lianglongwu17@mails.ucas.ac.cn (L.-w. Liang).

https://doi.org/10.1016/j.envpol.2019.113419
0269-7491/

certain hydrocarbons (Littman et al., 1956). During the fuel-burning process, however, large quantities of nitrogen oxides and hydrocarbons were released into the air, which resulted in the high ozone concentrations and severe rubber cracking observed in the Los Angeles (Haagen-Smit and Fox, 1956). Since then, scientists have focused on the relationships between ozone and its precursors. Using an observation-based model (OBM), Cardelino and Chameides studied the sensitivity of ozone concentrations in an urban atmosphere to changes in the emissions of ozone precursors (Cardelino and Chameides, 1995). Gao et al. (2017) adopted correlation analysis to study the relationship between ozone pollution and its precursors in Shanghai, identifying a negative correlation between the concentrations of ozone and nitrogen oxides. Yan et al. (2012) conducted a numerical simulation on the control of ozone pollution according to a two-dimensional air quality model. Their results indicated that the generation of ozone in Shenzhen resulted from the combined action of two precursor emissions, NO_x and volatile organic compounds (VOCs), the emission of VOCs having a relatively greater effect. The simulation indicated a synergistic emission reduction ratio of precursors that effectively reduced ozone pollution in Shenzhen. The factors influencing ozone pollution have also been studied globally. Abdul-Wahab et al. (2000) took the Shuaiba industrial district of Kuwait as their study area to analyze the relationship between the measured concentrations of ozone, nitrogen oxides, and non-methane hydrocarbons and meteorological factors, including air temperature, wind speed and direction, and solar radiation. Toh et al. (2013) found that meteorological conditions with low relative humidity, high temperature and low rainfall are beneficial to the formation of high levels of ozone. In addition, ozone concentration has been correlated with air pressure and wind direction. Lu et al. (2010) with the assistance of an OBM, explored the primary factors controlling ozone pollution in the Pearl River Delta in summer. A study by Loibi et al. (1994) showed that the ozone concentration over eastern Austria is higher than that over the central and western regions. Based on the rotated empirical orthogonal function (REOF), Cheng et al. (2018a) conducted a detailed analysis of ozone concentration. The authors divided their study area (China) into 12 regions and found that prevention of ozone pollution is urgently required in the regions of the North China Plain, the Huang-Huai Plain, the middle and lower reaches of the Yangtze River, the Pearl River Delta, and the Sichuan Basin. In addition, scholars have conducted different studies on the regional transportation of ozone pollution (Fiore et al., 2009; Zhang et al., 2008a; Zhang et al., 2009) and the relationship between ozone concentration and global climate change (Doherty et al., 2013; Solberg et al., 2005).

China is currently facing a serious problem of ozone pollution. In the air quality reports for 74 cities from July 2017, the average 8-h daily maximum ozone (O_3) concentration at the 90th percentile was 159 $\mu g/m^3$, growing by 12.8% per annum. The magnitude and frequency of high-ozone events in China are much greater than those in other industrialized regions such as Japan, South Korea, Europe, and the USA (Lu et al., 2018), while the North China Plain is the most polluted area in China (Li et al., 2019). JJJUA, with the most acute conflict between protecting ecological environment and sustaining economic development in China, showed a clear growth in ozone pollution. Air pollutant data for the region showed that for the period 2014–2017, the annual average concentrations of $PM_{2.5}$, PM_{10}, SO_2, and CO gradually decreased. Clear changes in NO_2 concentrations were not observable beyond a generally declining trend. In contrast, O_3 was the only pollutant with a continuously increasing annual average concentration, which is consistent with Silver's findings (Silver et al., 2018). Following $PM_{2.5}$, ozone has become the major secondary pollutant with significant negative effects on urban air quality (Peng et al., 2018). If no further studies are undertaken into ozone pollution, or the necessary measures to prevent and control it fail to be taken, ozone pollution will worsen, with serious consequences to follow. Most previous studies of ozone pollution in China, however, have been concentrated at the national scale (Silver et al., 2018), the Yangtze River Delta (Cheung and Wang, 2001; Li et al., 2017a; Wang et al., 2018; Xu et al., 2017), and the Pearl River Delta (Lu et al., 2010; Zhang et al., 2008b). There have been relatively few studies on ozone pollution across the JJJUA study region, although individual studies have been conducted on the capital city of Beijing (Cheng et al., 2018b; Xu et al., 2011). These studies have adopted mainly traditional methods, including time series and statistical and linear-regression analyses. In studying the influencing factors of ozone pollution, only a limited number of studies have focused on the interactions between the factors. Therefore, to address these knowledge gaps, this study analyzed the spatio-temporal evolution of ozone pollution and its influencing factors in the JJJUA using ozone data observed for 13 cities for the period 2014–2017. ArcGIS and SPSS software tools were applied to evaluate the data using Moran's I-based spatial autocorrelation test, Getis-Ord Gi*-based hot-spot analysis, and the innovative Geodetector methods. The objective of this study is to comprehensively explore the current status and characteristics of atmospheric pollution in the study region in order to provide a reference for investigating the mechanisms underlying the creation of atmospheric pollution as well as for the methods to mitigate it in the future.

2. Data sources and methods

2.1. Study region

The Beijing-Tianjin-Hebei Urban Agglomeration is surrounded by the Yanshan Mountains to the north, the Taihang Mountains to the west, the Bohai Sea to the east, and plains to the south. The terrain is high in the northwest and low in the southeast. It is dominated by plain landforms, supplemented by low mountains and coastal wetlands. The climate is a typical temperate semi-humid semi-arid continental monsoon, with distinct seasons and obvious dryness and humidity. Rainfall is concentrated mainly in the summer, with similar periods of rain and heat (Li et al., 2017b).

The JJJUA includes the political and cultural centers of China, which has made significant contributions to the rapid economic growth of the nation. It includes 13 cities at the prefecture level and above (Fig. 1): Beijing (BJ), Tianjin (TJ), Shijiazhuang (SJZ), Baoding (BD), Langfang (LF), Chengde (CD), Zhangjiakou (ZJK), Qinhuangdao (QHD), Handan (HD), Tangshan (TS), Hengshui (HS), Xingtai (XT), and Cangzhou (CZ). In total, they account for an area of 21.72×10^4 km^2, or 2.26% of China's total land surface. JJJUA, as one of the five national-level urban agglomerations, shows the acute contradiction between ecological environmental challenges and continued economic development (National Development and Reform Commission and Ministry of Environmental Protection, 2015). As a national key optimized functional area, along with the further promotion of the national strategy for coordinated development of Beijing-Tianjin-Hebei, its ecological and environmental issues have attracted wide public as well as academic attention. Severe regional atmospheric pollution is one barrier to the green and healthy development of the JJJUA.

2.2. Data sources

Ozone concentration data were obtained from the observed urban air quality data released in real time by the China National Environmental Monitoring Center. After removing the invalid sites, there were 75 monitoring sites as samples in 2014, 76 in 2015, 73 in

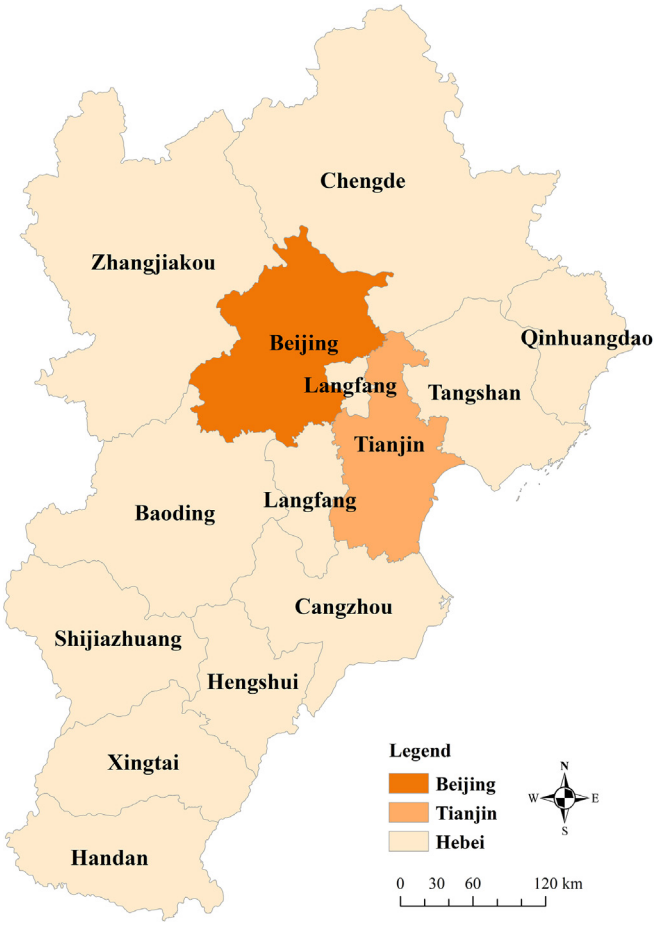

Fig. 1. Spatial range distribution of study area.

2016, and 72 in 2017. The valid numbers of days for the years 2014, 2015, 2016, and 2017 were 349, 364, 366, and 358, respectively. The arithmetic mean of the daily maximum 1-h average observed ozone concentrations for all sites in the inner city represented the pollution level of the city. These hourly data were combined to obtain daily maximum 1-h average (MDA1) ozone concentrations over the study period. According to the Ambient Air Quality Standard (AAQS) of GB3095-2012, the average daily maximum 8-h limit for O_3 concentration in a first-class environmental functional area is 100 μg/m^3, and the average hourly limit is 160 μg/m^3. The average daily maximum 8-h limit for O_3 concentration in a second-class environmental functional area is 160 μg/m^3, and the average hourly limit is 200 μg/m^3. In this study, the JJJUA is deemed a second-class environmental functional area.

Based on the national and international work described previously (Abdul-Wahab et al., 2000; Cai, 2012; Toh et al., 2013), we selected precipitation, sunshine duration, annual average temperature, evaporation, annual average wind speed, annual average air pressure, and annual average relative humidity as meteorological factors (Abdul-Wahab et al., 2000; Toh et al., 2013) and $PM_{2.5}$ and PM_{10} particulates (Cai, 2012) and the ozone precursors NO_2, CO, and SO_2 (Abdul-Wahab et al., 2000) as pollutant factors. The socioeconomic factors selected in this paper were: GDP, reflecting the economic development level; the proportion of secondary industry to GDP, reflecting the industrial structure; and the number of permanent residents, reflecting the population size (Liu et al., 2018). Daily meteorological data were obtained in 2017 from international exchange stations in the Beijing-Tianjin-Hebei region operated by the China Meteorological Data Network. The annual averages of temperature, relative humidity, average wind speed, air pressure, and the annual totals for precipitation, sunshine duration, and evaporation were calculated. Other atmospheric pollutant data were gathered from urban air quality observation data provided by the China National Environmental Monitoring Center. Data for 2017 were obtained from 72 observation stations in the 13 cities. The annual average concentrations of all pollutants at each observation station were calculated. The data for the influencing factors related to socioeconomic characteristics were obtained from the 2017 Statistical Bulletin of National Economic and Social Development.

2.3. Research methods

2.3.1. Evaluation of spatial agglomeration of ozone concentrations

(1) Spatial autocorrelation test of ozone concentration based on Moran's I

Distribution characteristics and spatial correlations can be described based on geography and spatial attributes. The spatial relevance characteristics of atmospheric activity result in similar regional ozone concentrations (Wang et al., 2015). This paper used Moran's I to measure the spatial autocorrelation of ozone concentration in the JJJUA, which is defined as follows (Getis and Ord, 1992):

$$I = \frac{n}{S_0} \frac{\sum_{i=1}^{n}\sum_{j=1}^{n} w_{i,j} z_i z_j}{\sum_{i=1}^{n} z_i^2} \tag{1}$$

where z_i represents the gap between the attribute value of element i and its average value ($x_i - \overline{X}$), $w_{i,j}$ is the spatial weight between the two elements i and j, and n represents the total number of elements. The equation for S_0 is as follows:

$$S_0 = \sum_{i=1}^{n}\sum_{j=1}^{n} w_{i,j} \tag{2}$$

The z_i score is calculated as follows:

$$z_i = \frac{I - E[I]}{\sqrt{V[I]}} \tag{3}$$

where

$$E[I] = -1/(n-1) \tag{4}$$

$$V[I] = E\left[I^2\right] - E[I]^2 \tag{5}$$

Usually, the range of I is between −1 and + 1 (inclusive of the two end points). A value of I less than 0 indicates a negative spatial correlation and a tendency toward dispersion. Lower values indicate stronger spatial negative correlations. In contrast, I equal to 0 represents a random spatial distribution, and a value of I greater than 0 indicates a positive spatial correlation and a clustering tendency. Larger values indicate stronger spatial positive correlations (Mitchell, 2005).

(2) Getis-Ord Gi*-based hot-spot analyses of ozone concentration

This tool is adopted to identify the spatial clustering with

statistically significant high values (hot spots) and low values (cold spots). By analyzing regional information, the spatial heterogeneity in the target area can be estimated. The formula used is as follows (Ord and Getis, 1995):

$$G_i^* = \frac{\sum_{j=1}^{n} w_{i,j}x_j - \overline{X}\sum_{j=1}^{n} w_{i,j}}{S\sqrt{\frac{\left[n\sum_{j=1}^{n} w_{i,j}^2 - \left(\sum_{j=1}^{n} w_{i,j}\right)^2\right]}{n-1}}} \quad (6)$$

where x_j represents the attribute value of element j, $w_{i,j}$ is the spatial weight between elements i and j; and n represents the total number of elements. In addition,

$$\overline{X} = \frac{\sum_{j=1}^{n} x_j}{n} \quad (7)$$

$$S = \sqrt{\frac{\sum_{j=1}^{n} x_j^2}{n} - (\overline{X})^2} \quad (8)$$

where Gi^* is the z-score. If Gi^* is significantly positive, the area has high value clustering (hot spot). Conversely, negative values indicate low value clustering (cold spot). The higher (or lower) the z-score, the more intense the clustering. A z-score near zero indicates no apparent spatial clustering (Mitchell, 2005).

2.3.2. Evaluation of the factors influencing ozone pollution

(1) Geodetector

The Geodetector, proposed by Wang et al. (2010), was first applied to recognize the environmental risk factors for diseases. As an important method for exploring and utilizing spatial heterogeneity and for revealing its driving forces (Wang and Xu, 2017), it has been applied to evaluating such widely diverse areas as the regional economy (Tan et al., 2016), land use (Ju et al., 2016; Ren et al., 2014), public health (Huang et al., 2014), meteorological observation (Ren et al., 2016), urban planning (Yang et al., 2016), the ecological environment (Luo et al., 2015; Todorova et al., 2016), agricultural production (Li et al., 2013), and tourism development (Wang et al., 2016). It can be used to probe numeric and explore qualitative data while also evaluating the interactions between two different elements, including strength, direction, and the linearity of relationships (Wang et al., 2016). This study applied the interaction detector to determine the interaction strength between different elements. We also used the differentiation and factor detector to examine the spatial differentiation of variables. All of the results are presented based on the q value. The principal equation for q is:

$$q = 1 - \frac{\sum_{h=1}^{L} N_h\sigma_h^2}{N\sigma^2} = 1 - \frac{SSW}{SST} \quad (9)$$

where h represents the hierarchy of variable Y or element X, N is the number of units, and σ^2 represents the variance in the value Y. The value of q is between 0 and + 1, with both endpoints included; therefore, the element or variable effect is reported as $100 \times q$ in percent. Larger values of q indicate a stronger effect by the element and explanatory power of the variable, and vice versa.

The interaction detector reveals whether the risk factors X_1 and X_2 have an interactive influence on the response variable Y, or whether these factors have independent effects on Y. The method of evaluation is to calculate the q values of the factors X_1 and X_2 on Y, respectively: $q(X_1)$ and $q(X_2)$, and then calculate the q value of their interaction: $q(X_1 \cap X_2)$, and compare $q(X_1)$, $q(X_2)$ and $q(X_1 \cap X_2)$. When $q(X_1 \cap X_2) < \text{Min}\ (q(X_1), q(X_2))$, the interaction results are nonlinear weakening. When $\text{Min}\ (q(X_1), q(X_2)) < q(X_1 \cap X_2) < \text{Max}\ (q(X_1), q(X_2))$, the results are unidirectional enhancement. When $q(X_1 \cap X_2) > \text{Max}\ (q(X_1), q(X_2))$, the results are bidirectional enhancement. When $q(X_1 \cap X_2) = q(X_1) + q(X_2)$, the results are independent of each other. When $q(X_1 \cap X_2) > q(X_1) + q(X_2)$, the results are nonlinear enhancement (Wang and Xu, 2017).

(2) Data preparation

ArcGIS inverse distance weighting (IDW) was applied to perform the spatial interpolation for the average concentrations of ozone and other pollutants, meteorological factors, and social and economic conditions in the JJJUA. The study region was divided into grids, and the average ozone concentration and the values of all influencing factors were extracted. With the assistance of the SPSS discrete tool, the values of all influencing factors were discretized. We entered the discretized results and the average ozone concentration into the Geodetector software to conduct the analyses (Wang and Xu, 2017).

3. Results

3.1. Temporal trends in ozone pollution in the JJJUA

3.1.1. Increasing annual average ozone concentrations for the period 2014–2017

The annual average ozone concentration in the JJJUA for the period 2014–2017 increased annually with widening amplification. Using the secondary standard limit, the annual mean MDA1 ozone concentration exceeding the standard also increased annually. In 2014, the annual mean MDA1 ozone concentration exceeded the standard by 2.58%, while in 2017 the increase soared by 13.13%. Among the 13 prefecture-level cities, the average annual ozone concentrations in Hengshui and Chengde decreased, while those in all other cities increased. Of all the cities, Tianjin, Qinhuangdao, Baoding, Zhangjiakou, Langfang, and Xingtai showed the fastest growth rates (Fig. 2).

For the period 2015–2017, the annual mean of the daily maximum 8-h average (MDA8) ozone concentration in the JJJUA decreased annually with widening amplification. Using the secondary standard limit, the annual mean MDA8 ozone concentration exceeding the standard declined. In 2015, the annual mean MDA8 ozone concentration exceeded the standard by 8.24%, while in 2017 the excess was only 1.96%. In the 13 prefecture-level cities, the annual mean MDA8 ozone concentration showed a slight increase only in Qinhuangdao, while the concentrations in all other cities declined, particularly in Beijing, Tangshan, Chengde, and Hengshui

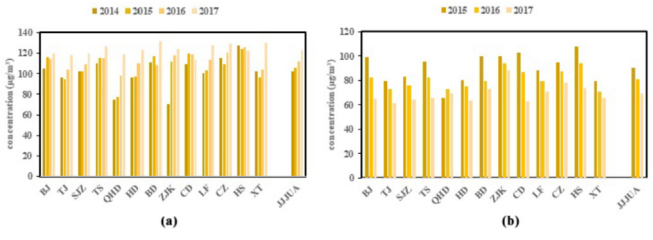

Fig. 2. Annual mean MDA1 and MDA8 ozone concentrations in cities of the JJJUA.

(Fig. 2).

The trend in annual mean MDA8 ozone concentration is completely opposite to that of the MDA1. Research has indicated that the effect on health of a high hourly ozone concentration in a day is larger than that of the MDA8, which significantly raises the risk of non-accidental deaths (Ban and Li, 2016). Therefore, MDA1 ozone concentrations were adopted for data analyses in this study.

3.1.2. Ozone concentration levels in spring and summer vs. autumn and winter

In 2017, except in winter (67 μg/m^3), ozone pollution appeared in the other three seasons in the JJJUA, especially in summer (183 μg/m^3), followed by spring (106 μg/m^3), with an aggravated trend in all seasons (Fig. 3c). Using the secondary standard limit, the MDA1 ozone concentrations in the spring, summer, and autumn of 2017 exceeded the standards by 9.78%, 40%, and 4.4%, respectively. The standard was not exceeded in winter.

3.1.3. Seasonality of monthly ozone concentrations

In 2017, monthly ozone concentrations during January to December in the JJJUA were all higher than in the same months in 2014. The inverted U curve (Fig. 3b) indicated that ozone pollution in the JJJUA from May to September was severe. The highest average ozone concentration occurred in June (206 μg/m^3), with a second peak in September (167 μg/m^3), while the lowest average concentration was in January (56 μg/m^3). Using the secondary standard limit, the mean MDA1 ozone concentration in June in the JJJUA showed the largest value in excess of the standard, 63.33%. The concentrations did not exceed the standard from January to April and October to December.

3.1.4. Daily characteristics of ozone pollution

In 2017, MDA1 ozone concentrations fluctuated in the JJJUA (Fig. 3a). From the last ten days of June to the first ten days of July, the MDA1 ozone concentration was relatively high, exceeding the limit set for a secondary environmental functional area. The peak MDA1 in 2017 was observed on May 28 (279 μg/m^3), while the minimum value occurred on January 1 (20 μg/m^3).

According to the weekly statistics, it was found that the ozone concentration in the region initially decreased, then increased, and later decreased again. Specifically, the concentrations decreased from Mondays to Tuesdays, and rapidly increased from Tuesdays to Fridays, during which time the concentrations started to accumulate and reached a peak on Fridays. Then the ozone concentration showed a declining trend, and reached the lowest levels on Sundays. Overall, ozone pollution on weekdays in the JJJUA in 2017 gradually worsened, while improving on the weekends; the average ozone concentrations on weekdays were higher than on weekends, which we term as the counter-weekend effect.

3.2. Spatial differentiation of ozone pollution

3.2.1. Contrasting average ozone concentrations in the central and southern vs. northern JJJUA

For the period 2014–2017, annual average ozone concentrations were higher in the central and southern regions of the study area and lower in the northern region (Fig. 4a). The highest annual average ozone concentrations were observed in Baoding, Cangzhou, and Xingtai, followed by Langfang and Tangshan, with values over 125 μg/m^3. Chengde had the lowest value (114 μg/m^3), indicating generally good air conditions.

Based on the ozone concentration standard (200 μg/m^3) for secondary environmental functional areas, the study area had 47 d where the ozone concentration exceeded the standard, equivalent to 13.13% in excess of the standard for the year. The highest percentage was 20.67% in Xingtai, followed by Tangshan, Langfang, Cangzhou and Handan, at over 15%. Beijing, Shijiazhuang, and Hengshui exceeded the standard by between 10% and 15%, while Tianjin, Qinhuangdao, Zhangjiakou, and Chengde exceeded the standard by less than 10%. Chengde had only 24 d that exceeded the standard (Fig. 4b).

3.2.2. Areal extent of ozone pollution in the summer of 2017

Comparing all seasons, summer had the widest areal scope of ozone pollution in 2017, followed by spring and autumn. No cities exceeded the standard in winter (Fig. 5). MDA1 ozone in summer exceeded the standard by 16.47–57.65%, with higher excesses in the central and southern regions than in the northern region. Of the cities, Xingtai exceeded the standard by the highest percentage, while Qinhuangdao exceeded it by the lowest (Fig. 5b). The range in

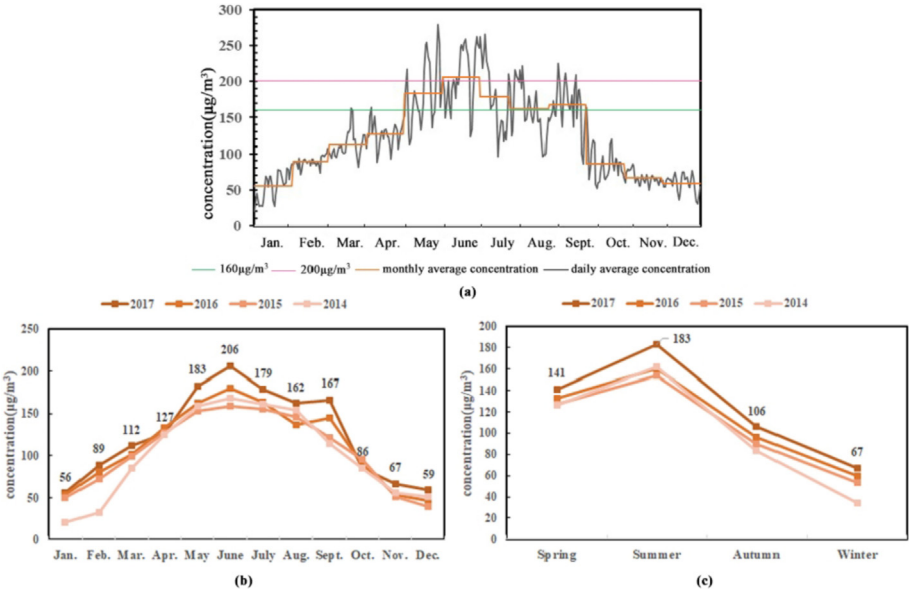

Fig. 3. Temporal characteristics of ozone concentration in the JJJUA, 2017.

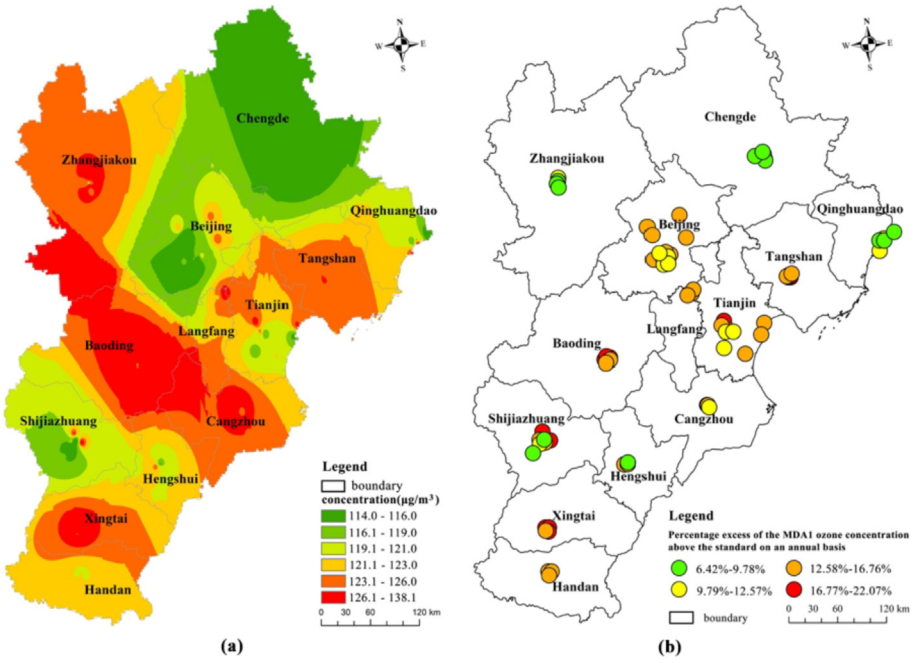

Fig. 4. (a) Spatial distribution of the annual average O_3 concentration and (b) excess of the percentage of the MDA1 ozone concentration above the standard in the JJJUA, 2017.

spring was 5.43−17.37%. Xingtai remained the city with the worst excesses above the standard, while Qinhuangdao was the city with the lowest (Fig. 5a). In autumn, the range was 1.10−17.58%; clearly, air quality improved and the scale of pollution decreased with better conditions in the northern region than in the southern region. The greatest percentage excess above the standard was in Baoding, while the lowest were in Tianjin, Zhangjiakou, and Chengde (Fig. 5c). MDA1 values for all cities in winter decreased to the standard value (Fig. 5d).

3.2.3. Areal extent of ozone pollution over different months in 2017

Monthly ozone concentration data for the JJJUA in 2017 showed that the areal extent of ozone pollution from January to April and October to December was quite small and that the percentages by which the MDA1 ozone concentrations exceeded the standard were all 0% (Fig. 6). Relatively high MDA1 ozone concentrations exceeding the standard were observed from May to September, with a widening pollution extent. In May, ozone pollution appeared in all the cities of the JJJUA. Xingtai and Handan, in the southern region, exceeded the standard the most, by 51.61% and 45.16%, respectively, followed by Shijiazhuang, Hengshui, Cangzhou, Baoding, Langfang, Beijing, and Tangshan in the central region, ranging from 35.48% to 38.71% in excess. Chengde, Zhangjiakou, Tianjin, and Qinhuangdao (Fig. 6e) had ozone concentrations only slightly exceeding the standard. Pollution increased in June, with all cities (except Chengde in the north) subject to an increase in ozone. Percentages in excess of the standard were over 40% in the central and southern regions; Xingtai (80%), Hengshui (76.67%), Baoding (73.33%), Langfang (66.67%), Cangzhou (63.33%), Handan (63.33%), Tangshan (60%), and Beijing (60%) were over 60% (Fig. 6f). From July to September, the pollution scope decreased and air quality improved. In July, ozone pollution above the standard increased in Zhangjiakou (41.67%) and Qinhuangdao (33.33%). All other cities showed a decrease in pollution, with the greatest decreases shown in Hengshui (12.5%) and Handan (20.83%) (Fig. 6g). In August, Hengshui showed a slight increase over the standard value, while those of other cities decreased. Except for Xingtai, the percentages above the standard remained lower than 40%, with the lowest rates in Zhangjiakou (6.45%) and Chengde (3.23%) (Fig. 6h). Excesses above the ozone standard increased in Tangshan, Qinhuangdao, Handan, Baoding, Chengde, Langfang, Cangzhou, and Hengshui in September, with the biggest change in Baoding (53.33%), which had the worst air quality. The percentages above the standard for all other cities remained under 40% (Fig. 6i).

3.2.4. Significant positive spatial correlations of ozone concentration

(1) Significant positive spatial correlations of ozone pollution, especially in summer and autumn

Using the spatial autocorrelation analysis tool in ArcGIS, we tested annual, seasonal, and monthly average ozone concentrations for 72 observation stations in the JJJUA in 2017. Generally, $Z(I) < -2.58$ or $> +2.58$ and $p < 0.01$ indicate that the confidence coefficient is 99%; $Z(I) < -1.96$ or $> +1.96$ and $p < 0.05$ indicate that the confidence coefficient is 95%; and $Z(I) < -1.65$ or $> +1.65$ and $p < 0.1$ indicate that the confidence coefficient is 90%. Our results show only positive values for Moran's I. The Z(I) for all months, excluding February and March, exceeded 1.96, while p was lower than 0.05, which passed the significance test of 5%. These statistical parameters indicate that there was a significant positive spatial correlation for ozone pollution in JJJUA, especially in summer and autumn (Table 1).

(2) Hot spots in Baoding and Xingtai and cold spots in Beijing and Chengde

The annual Z(I) value was 4.35, which suggested a clear spatial agglomeration. Hot spots were concentrated in Baoding and Xingtai, which had relatively stable and continuous ozone pollution. Cold spots occurred mainly in Beijing and Chengde, where ozone pollution was not serious. Spatial autocorrelations of ozone for the other prefecture-level cities were not evident.

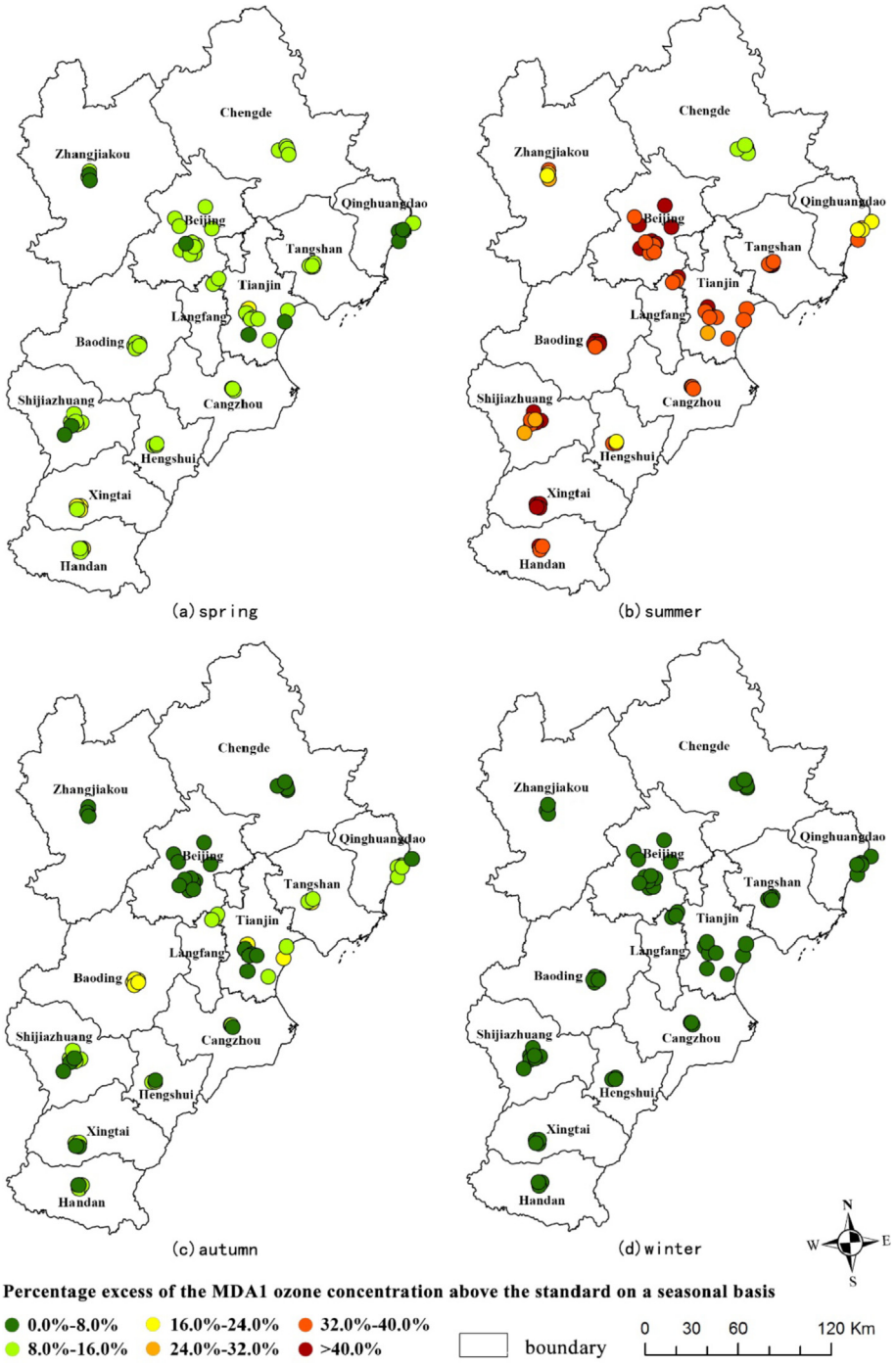

Fig. 5. Spatial distribution of seasonal average O_3 concentrations plotted as percentages exceeding the standard concentration limit in the JJJUA, 2017.

(3) Beijing showed good air quality based on ozone pollution levels, which was relatively stable and continuous

Seasonally, hot spots in spring were concentrated in Langfang and Cangzhou, while cold spots were concentrated in Beijing and Qinhuangdao. In summer, hot spots were concentrated in the south, e.g., Baoding and Xingtai, while cold spots were found in Chengde and Qinhuangdao. Hot spots in autumn were distributed in Baoding and Qinhuangdao, while cold spots were distributed in Beijing, Chengde, and Shijiazhuang. Hot spots in winter were concentrated in the north, in Zhangjiakou and Chengde, while cold spots were concentrated in Beijing and Shijiazhuang. Beijing generally showed good air quality in terms of ozone pollution, which remained relatively stable and continuous.

(4) Characteristics of spatial agglomeration of monthly ozone concentrations

On a monthly basis, hot spots in January were concentrated in cities located in the northern part of the urban agglomeration, such as Zhangjiakou, Chengde, and Qinhuangdao, while cold spots were located in cities in the southern region, such as Shijiazhuang and

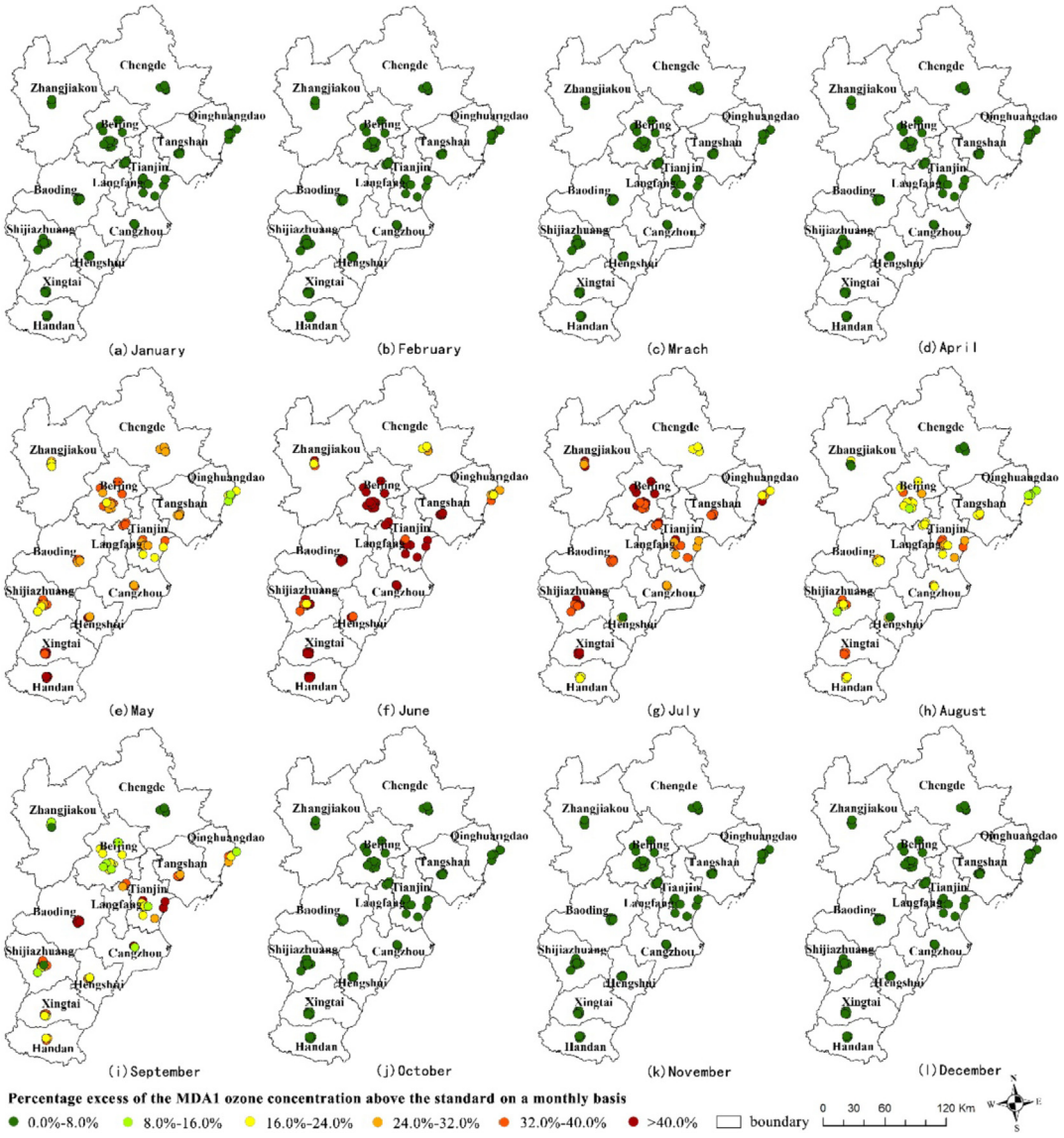

Fig. 6. Spatial distribution of average monthly O_3 concentrations plotted as percentages exceeding the standard concentration limit in the JJJUA, 2017.

Table 1
Spatial autocorrelation indices for annual, seasonal, and monthly ozone concentrations in the JJJUA, 2017.

Time	Year	Spr.	Sum.	Aut.	Win.	Jan.	Feb.	Mar.	Apr.	May	June	July	Aug.	Sept.	Oct.	Nov.	Dec.
Moran's I	0.38	0.21	0.68	0.57	0.43	0.52	0.09	0.15	0.32	0.57	0.58	0.55	0.71	0.73	0.72	0.6	0.48
Z(I)	4.35	2.52	7.65	6.55	5.17	6.11	1.16	1.9	3.78	6.43	6.55	6.27	8.06	8.19	8.14	6.6	5.4

Xingtai. There was no obvious spatial aggregation feature in February. In March, hot spots were found in the south, distributed mainly in Tianjin, while cold spots were distributed in the north, i.e., in Beijing and Shijiazhuang. In April, hot spots were found in Chengde and Cangzhou, while cold spots remained in Beijing and Shijiazhuang. In May, hot spots expanded to the south, distributed across Baoding, Xingtai, and Handan, and cold spots moved further to the west and east, mainly in Zhangjiakou and Qinhuangdao. In June, spatial agglomeration became more remarkable, and hot spots occurred in Shijiazhuang and Xingtai, while cold spots expanded to the north, concentrated mainly in Zhuangjiakou, Qinhuangdao, and Chengde. In July, Beijing and Shijiazhuang became agglomeration areas for hot spots, and cold spots expanded southward, distributed mainly in Hengshui, Handan, and Chengde. In August, Baoding and Xingtai again became agglomeration areas for hot spots. In September, hot spots moved northward, mainly in Baoding and Tangshan, while cold spots occurred mainly in Beijing, Zhangjiakou, and Chengde. In October, hot spots were concentrated mainly in Zhangjiakou, Qinhuangdao, and Cangzhou, while cold spots were concentrated mainly in Beijing and Shijiazhuang. In November and December hot spots occurred in Zhangjiakou and cold spots occurred primarily in Beijing and Shijiazhuang.

3.3. Factors influencing ozone pollution in the JJJUA

3.3.1. Exploring the influencing factors

The Geodetector was used in this study to identify the factors influencing ozone pollution in the JJJUA. The q values obtained using the factor detector of factors ranked as follows: PM_{10} concentration (0.509) > NO_2 concentration (0.43) > CO concentration (0.425) > average wind speed (0.417) > sunshine duration (0.353) > evaporation (0.35) > precipitation (0.254) > annual average temperature (0.244) > $PM_{2.5}$ concentration (0.226) > SO_2 concentration (0.221). The effects of air pressure, relative humidity, GDP, the proportion of secondary industry (TPOSI), and the population were not significant. Therefore, concentrations of PM_{10}, NO_2, and CO, as well as average wind speed, sunshine duration, and evaporation had relatively large effects on ozone pollution, while precipitation, annual average temperature, $PM_{2.5}$ concentration, and SO_2 concentration had relatively small effects.

(1) Impact of other pollutants on ozone pollution

The monthly variations in atmospheric particulate (PM_{10}, $PM_{2.5}$) concentrations were completely opposite to that of ozone pollution. The highest particulate matter concentrations were found in winter, while ozone concentrations were relatively low. In summer, particulate matter pollution declined, while ozone pollution increased. Under certain conditions, high concentrations of particulates lead to an increase in aerosol optical thickness, weakening the photochemical generation rate of ozone and reducing the ozone concentration. In addition, the ozone concentration is affected by heterogeneous chemical processes occurring on the surface of particulates (Cai, 2012). Increasing $PM_{2.5}$ concentrations can weaken atmospheric radiation such that it suppresses ozone levels by extinction of ultraviolet rays (Jia et al., 2017).

As important precursor substances to ozone formation, the concentrations of NO_2 and CO were quite high in winter but low in summer, and their temporal variations were opposite to those of ozone. This situation occurred because the relevant photochemical reactions usually occur in summer. Under certain conditions, NO_x, NO, and VOCs generate ozone through photochemical reactions, which increases the ozone concentration and drives higher ozone pollution. In autumn and winter, due to increases in pollutant emissions and frequent inversions, atmospheric stratification is relatively stable, which is not conducive to local transport of pollutants or to dilution and diffusion. On the other hand, the low temperature and weak solar radiation in winter are not conducive to photochemical reactions. As a result, NO_2 and CO accumulate, resulting in relatively high concentrations of these molecules in winter (Cao et al., 2017). There is a certain relationship between the photochemical oxidation of SO_2 and O_3. A high ozone concentration greatly promotes the chemical conversion of sulfur dioxide to sulfate (Liu et al., 2001).

(2) Impact of meteorological factors on ozone pollution

Meteorological factors play an important role in affecting the ozone concentration near the ground, but the dominant factors are different in different situations and regions (Xu and Zhu, 1994). The results presented in this paper show that wind speed, sunshine duration, evaporation, precipitation, and temperature were the main influencing factors of ozone pollution in the JJJUA. Wind speed also affects ozone pollution by transporting and cleaning air pollutants out of the study areas (Cao et al., 2017; Dueñas et al., 2002; Gautam and Srivastava, 2017). Sunshine duration and evaporation are related to solar radiation. Generally, strong solar radiation drives active photochemical reactions, which increases ozone pollution and explains the higher ozone concentrations in spring and summer than in autumn and winter (Wang et al., 2017). Precipitation affects mainly ozone pollution by scouring aerosol particles (Toh et al., 2013). High temperatures can enhance solar radiation and reduce cloudiness, thus increasing the intensity of photochemical reactions, resulting in an increase in ozone concentration (Cao et al., 2017). Biogenic emissions of ozone precursors also increase with temperature, which favors ozone formation (Struzewska and Jefimow, 2016).

3.3.2. Exploring the interactions between different factors

Using the interactive detection module to analyze the influencing factors, we found that interactions between the influencing factors strengthened ozone pollution. Among all interactions, nonlinear enhancements were found for the following interaction combinations: NO_2 concentration and relative humidity; CO concentration and relative humidity; $PM_{2.5}$ concentration and SO_2 concentration, wind speed, sunshine duration, relative humidity, and evaporation; SO_2 concentration and wind speed, precipitation, sunshine duration, relative humidity, and evaporation; precipitation and relative humidity; temperature and air pressure, relative humidity; air pressure and relative humidity; and sunshine duration and relative humidity. Interactions between the socioeconomic factors and other factors also showed a nonlinear enhancement, and all other interactions resulted in a bidirectional enhancement. In summary, the influencing factors on ozone pollution were connected and were not completely independent; when an interaction combination was applied, the explanatory power of the variable increased. In all interactive relationships (Table 2), the interactions between wind speed, sunshine duration, and concentrations of $PM_{2.5}$, PM_{10}, and SO_2 were the strongest, with a q value larger than 0.7. Therefore, the interaction of meteorological factors, such as wind speed and sunshine duration and other pollutant factors, was a vital factor influencing ozone pollution. The interactions between TPOSI and the concentrations of NO_2, $PM_{2.5}$, and PM_{10} were much stronger than the effect of TPOSI itself, with a q value greater than 0.6, which indicated that the effects of secondary industry on ozone pollution were closely related to the emission of pollutants such as NO_2, $PM_{2.5}$, and PM_{10}.

4. Discussion and conclusions

In the Beijing-Tianjin-Hebei region, the average ozone concentration increased annually, with rapid changes from 2014 to 2017. In the 13 prefecture-level cities, all except Hengshui and Chengde showed a rising annual average ozone concentration, and Tianjin, Qinhuangdao, Baoding, Zhangjiakou, Langfang, and Xingtai showed the fastest increases. From a seasonal perspective, ozone pollution was worse in spring and summer than in autumn and winter. In terms of monthly variation, an inverted U-shaped pattern for the change in average ozone concentration was observed in the region. The period from May to September showed elevated levels of ozone pollution; the ozone concentration was highest in June and lowest in January. Daily average data indicated that ozone pollution fluctuated regularly. From the last ten days of June to the first ten days of July, the MDA1 ozone concentrations exceeded the limit set for second-class environmental functional areas. The average ozone concentration on workdays was higher than that on non-workdays, showing a counter-weekend effect. Furthermore, ozone pollution on weekdays worsened, while that on non-workdays improved.

A detailed analysis of the annual average ozone concentration in 2017 showed that the central and southern parts of the study region had high ozone concentrations, while the northern regions had lower values. The highest annual average ozone concentration

Table 2
The q values for interactions between factors influencing ozone pollution in the JJJUA, 2017.

	NO_2	CO	$PM_{2.5}$	PM_{10}	SO_2	Wind speed	Precipitation	Temperature	Pressure	Sunshine duration	Relative humidity	Evaporation	GDP	TPOSI	Population
NO_2	0.43														
CO	0.57	0.43													
$PM_{2.5}$	0.60	0.66	0.23												
PM_{10}	0.67	0.69	0.59	0.51											
SO_2	0.57	0.57	0.53	0.58	0.22										
Wind speed	0.68	0.69	**0.72**	**0.70**	**0.74**	0.42									
Precipitation	0.58	0.62	0.43	0.60	0.50	0.56	0.25								
Temperature	0.52	0.63	0.41	0.59	0.46	0.57	0.33	0.24							
Pressure	0.48	0.49	0.32	0.58	0.36	0.55	0.42	0.48	0.18						
Sunshine duration	0.63	0.64	**0.71**	**0.71**	**0.75**	0.59	0.55	0.55	0.51	0.35					
Relative humidity	0.56	0.53	0.68	0.61	0.55	0.44	0.52	0.50	0.48	0.56	0.11				
Evaporation	0.59	0.56	0.66	0.66	0.63	0.55	0.54	0.51	0.44	0.48	0.42	0.35			
GDP	0.53	0.49	0.30	0.56	0.38	0.54	0.34	0.39	0.26	0.49	0.26	0.46	0.05		
TPOSI	0.64	0.55	0.67	0.68	0.47	0.60	0.57	0.58	0.46	0.56	0.35	0.45	0.20	0.15	
Population	0.60	0.59	0.37	0.61	0.47	0.58	0.37	0.38	0.34	0.51	0.46	0.57	0.20	0.43	0.12

occurred in Baoding, Cangzhou, and Xingtai, followed by Langfang and Tangshan. Chengde had the lowest annual average ozone concentration. According to the range of seasonal MDA1 values for the study region, we found that the scope of ozone pollution over the standard limit in 2017 was widest in summer, followed by spring and autumn. The ozone concentration in winter did not exceed the standard in any cities studied. Monthly data for ozone pollution in 2017 were also analyzed spatially, and the periods from January to April and October to December showed limited areas of pollution, although the scope widened from May to September. There was a significant positive spatial correlation in ozone pollution, with the most significant correlation occurring in summer and autumn. Hot spots were distributed mainly in Baoding and Xintai, which were relatively stable for these continuously polluted cities, while cold spots were distributed in Beijing and Chengde, which had good air quality.

Using Geodetector, the factors influencing ozone pollution in 2017 were identified. The precursors of ozone, i.e., high concentrations of NO_2, CO, PM_{10}, $PM_{2.5}$, and SO_2, average wind speed, sunshine duration, evaporation, precipitation, and temperature had a significant influence on ozone pollution. The interactions between all influencing factors were analyzed via an interactive detection module. We found that the interactions between the factors influencing ozone pollution produced positive feedback, and the combined action of meteorological factors such as wind speed, sunshine duration, and other pollutant elements was a major influencing factor. Finally, the effects of secondary industry on ozone pollution were found to be closely related to the emission of pollutants such as NO_2, $PM_{2.5}$, and PM_{10}.

5. Study limitations and future prospects

While important results were obtained in this study, three important points need to be addressed in any future research.

(1) Variations in the MDA8 annual concentrations in the JJJUA from 2015 to 2017 were opposite to those of the annual MDA1 O_3 concentrations. The reasons for this are unclear and should be explored in the future with additional data.
(2) When analyzing the influencing factors, due to a shortage of data for VOCs, topography and altitude, and vehicle inventory, we could not explore the magnitude of the influence of these three factors on ozone pollution, and their relationships. Based on current research, these three elements appear to be the important influencing factors in the formation of ozone pollution.
(3) It is difficult to interpret the mechanisms influencing the formation and development of ozone pollution in the Beijing-Tianjin-Hebei region. Additional specialized knowledge in other disciplines should be applied to address this issue.

Declaration of competing interest

The authors declare that there is no conflict of interest.

Acknowledgments

This study was funded by the Major Program of the National Natural Science Foundation of China (No. 41590842) and Open Fund Project of New Urbanization Research Institute of Tsinghua University (TUCSU—K—17015—01).

References

Abdul-Wahab, S., Bouhamra, W., Ettouney, H., Sowerby, B., Crittenden, B.D., 2000. Analysis of ozone pollution in the Shuaiba industrial area in Kuwait. Int. J. Environ. Stud. 57, 207–224.
Adams, W.C., 1987. Effects of ozone exposure at ambient air pollution episode levels on exercise performance. Sport. Med. 4, 395–424.
Ban, J., Li, T.T., 2016. Short-term effects of different ozone metrics on daily mortality in Beijing. J. Environ. Health 33, 287–291.
Cai, Y.F., 2012. Observation and Numerical Modeling on the Interaction between Atmospheric Particulate and Ozone in Urban Area of Yangtze River Delta. Nanjing University.
Cao, T.W., Wu, K., Kang, P., Wen, X.H., Li, H., Li, A.Q., Lv, X.Y., Wang, Y., Pan, W.H., Fan, W.B., Yi, R., Bao, X.B., He, M.Q., 2017. Study on ozone pollution characteristics and meteorological cause of Chengdu – Chongqing Urban Agglomeration. Acta Sci. Circumstantiae 38, 1275–1284.
Cardelino, C.A., Chameides, W.L., 1995. An observation-based model for analyzing ozone precursor relationships in the urban atmosphere. J. Air Waste Manag. Assoc. 45, 161–180.
Chameides, W.L., Kasibhatla, P.S., Yienger, J., Levy, H., 1994. Growth of continental-scale metro-agro-plexes, regional ozone pollution, and world food production. Science 264, 74–77.
Cheng, L.J., Wang, S., Gong, Z.Y., Li, H., Yang, Q., Wang, Y.Y., 2018a. Regionalization based on spatial and seasonal variation in ground-level ozone concentrations across China. J. Environ. Sci. 67, 179–190.
Cheng, N., Chen, Z., Sun, F., Sun, R., Dong, X., Xie, X., Xu, C., 2018b. Ground ozone concentrations over Beijing from 2004 to 2015: variation patterns, indicative precursors and effects of emission-reduction. Environ. Pollut. 237, 262–274.
Cheung, V.T.F., Wang, T., 2001. Observational study of ozone pollution at a rural site in the Yangtze Delta of China. Atmos. Environ. 35, 4947–4958.
Cooper, O.R., Parrish, D.D., Ziemke, J., Balashov, N.V., Cupeiro, M., Galbally, I.E., et al., 2014. Global distribution and trends of tropospheric ozone: an observation-based review. Elem. Sci. Anth. 2, 1–28.

Doherty, R.M., Wild, O., Shindell, D.T., Zeng, G., MacKenzie, I.A., Collins, W.J., et al., 2013. Impacts of climate change on surface ozone and intercontinental ozone pollution: a multi-model study. J. Geophys. Res. Atmos. 118, 3744–3763.
Dueñas, C., Fernández, M.C., Cañete, S., Carretero, J., Liger, E., 2002. Assessment of ozone variations and meteorological effects in an urban area in the Mediterranean Coast. Sci. Total Environ. 299, 97–113.
Feng, Z.Z., Hu, E.Z., Wang, X.K., Jiang, L.J., Liu, X.J., 2015. Ground-level O_3 pollution and its impacts on food crops in China: a review. Environ. Pollut. 199, 42–48.
Fiore, A.M., Dentener, F.J., Wild, O., Cuvelier, C., Schultz, M.G., Hess, P., et al., 2009. Multimodel estimates of intercontinental source-receptor relationships for ozone pollution. J. Geophys. Res. 114, 83–84.
Friend of Nature, 2001. Environmental Warnings of the 20th Century. Huaxia Publishing House, Beijing.
Gao, W., Tie, X.X., Xu, J.M., Huang, R.J., Mao, X.Q., Zhou, G.Q., Chang, L.Y., 2017. Long-term trend of O_3 in a mega City (Shanghai), China: characteristics, causes, and interactions with precursors. Sci. Total Environ. 603–604, 425–433.
Gautam, P., Srivastava, R.K., 2017. Assessment of ozone variations and meteorological effects in an urban area in the Jabalpur region. Afr. J. Sci. Technol. 8, 4949–4953.
Getis, A., Ord, J.K., 1992. The analysis of spatial association by use of distance statistics. Geogr. Anal. 24, 189–206.
Haagen-Smit, A.J., Fox, M.M., 1956. Ozone formation in photochemical oxidation of organic substances. J. Immunol. 48, 2086–2089.
Huan, L., Liu, S., Xue, B., Lv, Z.F., Meng, Z.H., Yang, X.F., Xue, T., Yu, Q., He, K., 2018. Ground-level ozone pollution and its health impacts in China. Atmos. Environ. 173, 223–230.
Huang, J.X., Wang, J.F., Bo, Y.C., Xu, C.D., 2014. Identification of health risks of hand, foot and mouth disease in China using the geographical detector technique. Int. J. Environ. Res. Public Health 11, 3407–3423.
Jia, M.W., Zhao, T.L., Cheng, X.H., Gong, S.L., Zhang, X.Z., Tang, L.L., Liu, D.Y., Wu, X.H., Wang, L.M., Chen, Y.S., 2017. Inverse relations of $PM_{2.5}$ and O_3 in air compound pollution between cold and hot seasons over an urban area of east China. Atmosphere 8, 1–12.
Ju, H.R., Zhang, Z.X., Zuo, L.J., Wang, J.F., Zhang, S.R., Wang, X., Zhao, X.L., 2016. Driving forces and their interactions of built-up land expansion based on the geographical detector: a case study of Beijing, China. Int. J. Geogr. Inf. Sci. 30, 2188–2207.
Lefohn, A.S., Malley, C.S., Simon, H., Wells, B., Xu, X., Zhang, L., Wang, T., 2016. Responses of human health and vegetation exposure metrics to changes in ozone concentration distributions in the European Union, United States, and China. Atmos. Environ. 152, 123–145.
Li, K., Jacob, D.J., Liao, H., Shen, L., Zhang, Q., Bates, K.H., 2019. Anthropogenic drivers of 2013–2017 trends in summer surface ozone in China. Proc. Natl. Acad. Sci. 116, 422–427.
Li, K.W., Chen, L.H., Ying, F., White, S.J., Jang, C., Wu, X.C., Gao, X., Hong, S.M., Shen, J.D., Azzi, M., Cen, K., 2017a. Meteorological and chemical impacts on ozone formation: a case study in Hangzhou, China. Atmos. Res. 196, 40–52.
Li, X.W., Xie, Y.F., Wang, J.F., Christakos, G., Si, J.L., Zhao, H.N., Ding, Y.Q., Li, J., 2013. Influence of planting patterns on fluoroquinolone residues in the soil of an intensive vegetable cultivation area in north China. Sci. Total Environ. 458–460, 63–69.
Li, Z., Sun, R.H., Zhang, J.C., Zhang, C., 2017b. Temporal-spatial analysis of vegetation coverage dynamics in Beijing-Tianjin-Hebei metropolitan regions. Acta Ecol. Sin. 37, 7418–7426.
Littman, F.E., Ford, H.W., Endow, N., 1956. formation of ozone in the Los Angeles atmosphere. JAPCA 6, 171–175.
Liu, H.M., Fang, C.L., Huang, J.J., Zhu, X.D., Zhou, Y., Wang, Z.B., Zhang, Q., 2018. The spatial-temporal characteristics and influencing factors of air pollution in Beijing-Tianjin-Hebei urban agglomeration. Acta Geograph. Sin. 73, 177–191.
Liu, H.N., Jiang, W.M., Tang, J.P., Li, X., 2001. A numerical study on the troposphere photochemical oxidation process of sulfur dioxide over China. Acta Sci. Circumstantiae 3, 358–363.
Loibi, W., Winiwarter, W., Kopsca, A., Zufger, J., Baumann, R., 1994. Estimating the spatial distribution of ozone concentrations in complex terrain. Atmos. Environ. 28, 2557–2566.
Lu, K.D., Zhang, Y.H., Su, H., Shao, M., Zeng, L.M., Zhong, L.J., Xiang, Y.R., Chang, C.C., Chou, C.K., Charles, Wahner A., 2010. Regional ozone pollution and key controlling factors of photochemical ozone production in Pearl River Delta during summer time. Sci. China Chem. 53, 651–663.
Lu, X., Hong, J.Y., Zhang, L., Cooper, O.R., Schultz, M.G., Xu, X.B., Wang, T., Gao, M., Zhao, Y.H., Zhang, Y.H., 2018. Severe surface ozone pollution in China: a global perspective. Environ. Sci. Technol. Lett. 5, 487–494.
Luo, W., Jasiewicz, J., Stepinski, T., Wang, J.F., 2015. Spatial association between dissection density and environmental factors over the entire conterminous United States. Geophys. Res. Lett. 43, 692–700.
Mitchell, A., 2005. The ESRI Guide to GIS Analysis, vol. 2. ESRI Press, Redlands, California, USA.
National Development and Reform Commission and Ministry of Environmental Protection, 2015. Beijing-Tianjin-Hebei Coordinated Development of Eco-Environmental Protection Planning. Beijing.
Ord, J.K., Getis, A., 1995. Local spatial autocorrelation statistics: distributional issues and an application. Geogr. Anal. 27, 286–306.
Peng, C., Liao, Y.L., Zhang, N.X., 2018. Temporal and spatial distribution of ozone pollution in Chinese urban agglomerations. Geo Inf. Sci. 20, 57–67.
Ren, Y., Deng, L.Y., Zuo, S.D., Luo, Y.J., Shao, G.F., Wei, X.H., Hua, L.Z., Yang, Y.S., 2014. Geographical modeling of spatial interaction between human activity and forest connectivity in an urban landscape of southeast China. Landsc. Ecol. 29, 1741–1758.
Ren, Y., Deng, L.Y., Zuo, S.D., Song, X.D., Liao, Y.L., Xu, C.D., Chen, Q., Hua, L.Z., Li, Z.W., 2016. Quantifying the influences of various ecological factors on land surface temperature of urban forests. Environ. Pollut. 216, 519–529.
Silver, B., Reddington, C.L., Arnold, S.R., Spracklen, D.V., 2018. Substantial changes in air pollution across China during 2015–2017. Environ. Res. Lett. 13, 1–8.
Solberg, S., Derwent, R.G., Hov, O., Langner, J., Lindskog, A., 2005. European abatement of surface ozone in a global perspective. AMBIO A J. Hum. Environ. 34, 47–53.
Struzewska, J., Jefimow, M., 2016. A 15-year analysis of surface ozone pollution in the context of hot spells episodes over Poland. Acta Geophys. 64, 1875–1902.
Tai, A.P.K., Martin, M.V., Heald, C.L., 2014. Threat to future global food security from climate change and ozone air pollution. Nat. Clim. Chang. 4, 817–821.
Tan, J.T., Zhang, P.Y., Lo, K., Li, J., 2016. The urban transition performance of resource-based cities in Northeast China. Sustainability 8, 1022.
Todorova, Y., Lincheva, S., Yotinov, I., Topalova, Y., 2016. Contamination and ecological risk assessment of long-term polluted sediments with heavy metals in small hydropower cascade. Water Resour. Manag. 30, 4171–4184.
Toh, Y.Y., Lim, S.F., Glasow, R.V., 2013. The influence of meteorological factors and biomass burning on surface ozone concentrations at Tanah Rata, Malaysia. Atmos. Environ. 70, 435–446.
Wang, J.F., Li, X.H., Christakos, G., Liao, Y.L., Zhang, T., Gu, X., Zheng, X.Y., 2010. Geographical detectors-based health risk assessment and its application in the neural tube defects study of the Heshun region, China. Int. J. Geogr. Inf. Sci. 24, 107–127.
Wang, J.F., Xu, C.D., 2017. Geodetector: principle and prospective. Acta Geograph. Sin. 72, 116–134.
Wang, T., Xue, L., Brimblecombe, P., Lam, Y.F., Li, L., Zhang, L., 2017. Ozone pollution in China: a review of concentrations, meteorological influences, chemical precursors, and effects. Sci. Total Environ. 575, 1582–1596.
Wang, X.G., Xi, J.C., Yang, D.Y., Tian, C., 2016. Spatial differentiation of rural tourism and its determinants in China: a geo-detector-based case study of Yesanpo scenic area. J. Resour. Ecol. 7, 464–471.
Wang, Y.Y., Du, H.Y., Xu, Y.Q., Lu, D.B., Wang, X.Y., Guo, Z.Y., 2018. Temporal and spatial variation relationship and influence factors on surface urban heat island and ozone pollution in the Yangtze River Delta, China. Sci. Total Environ. 631–632, 921–933.
Wang, Z.B., Fang, C.L., Xu, G., Pan, Y.P., 2015. Spatial-temporal characteristics of the $PM_{2.5}$ in China in 2014. Acta Geograph. Sin. 70, 1720–1734.
Xu, J., Ma, J.Z., Zhang, X.L., Xu, X.B., Xu, X.F., Lin, W.L., Wang, Y., Meng, W., Ma, Z.Q., 2011. Measurements of ozone and its precursors in Beijing during summertime: Impact of urban plumes on ozone pollution in downwind rural areas. Atmos. Chem. Phys. 11, 12241–12252.
Xu, J.L., Zhu, Y.X., 1994. Effects of the meteorological factors on the ozone pollution near the ground. Chin. J. Atmos. Sci. 18, 751–757.
Xu, Z.N., Huang, X., Nie, W., Chi, X.G., Xu, Z., Zheng, L.F., Sun, P., Ding, A.J., 2017. Influence of synoptic condition and holiday effects on VOCs and ozone production in the Yangtze River Delta region, China. Atmos. Environ. 168, 112–124.
Yan, M., Yin, K.H., Liang, Y.X., Zhuang, Y.X., Liu, B.Z., Li, J.L., Liu, C.F., 2012. Ozone pollution in summer in Shenzhen city. Res. Environ. Sci. 25, 411–418.
Yang, K., Huang, Y.Y., Shi, F., Fan, W.J., Zhou, G.M., 2018. Research on the ozone pollution and control measures in US and Japan. Chin. J. Envir. Manag. 10, 85–90.
Yang, R., Xu, Q., Long, H.L., 2016. Spatial distribution characteristics and optimized reconstruction analysis of China's rural settlements during the process of rapid urbanization. J. Rural Stud. 47, 413–424.
Zhang, L., Jacob, D.J., Boersma, K.F., Jaffe, D.A., Olson, J.R., Bowman, K.W., et al., 2008a. Transpacific transport of ozone pollution and the effect of recent Asian emission increases on air quality in North America: an integrated analysis using satellite, aircraft, ozonesonde, and surface observations. Atmos. Chem. Phys. 8, 6117–6136.
Zhang, L., Jacob, D.J., Kopacz, M., Henze, D.K., Singh, K., Jaffe, D.A., 2009. Intercontinental source attribution of ozone pollution at western U.S. sites using an adjoint method. Geophys. Res. Lett. 36, 245–253.
Zhang, Y.H., Su, H., Zhong, L.J., Cheng, Y.F., Zeng, L.M., Wang, X.S., Xiang, Y.R., Wang, J.F., Gao, D.F., Shao, M., Fan, S.J., Liu, S.C., 2008b. Regional ozone pollution and observation-based approach for analyzing ozone–precursor relationship during the PRIDE-PRD2004 campaign. Atmos. Environ. 42, 6203–6218.